
Fake It Till You Make It: Near-Distribution Novelty Detection by Score-Based Generative Models

Hossein Mirzaei
Sharif University of Technology

Mohammadreza Salehi
University of Amsterdam

Sajjad Shahabi
Sharif University of Technology

Efstratios Gavves
University of Amsterdam

Cees G. M. Snoek
University of Amsterdam

Mohammad Sabokrou
Institute for Research in Fundamental Sciences (IPM)

Mohammad Hossein Rohban
Sharif University of Technology

Abstract

We aim for image-based novelty detection. Despite considerable progress, existing models either fail or face a dramatic drop under the so-called “near-distribution” setting, where the differences between normal and anomalous samples are subtle. We first demonstrate existing methods experience up to 20% decrease in performance in the near-distribution setting. Next, we propose to exploit a score-based generative model to produce synthetic near-distribution anomalous data. Our model is then fine-tuned to distinguish such data from the normal samples. We provide a quantitative as well as qualitative evaluation of this strategy, and compare the results with a variety of GAN-based models. Effectiveness of our method for both the near-distribution and standard novelty detection is assessed through extensive experiments on datasets in diverse applications such as medical images, object classification, and quality control. This reveals that our method considerably improves over existing models, and consistently decreases the gap between the near-distribution and standard novelty detection performance. Overall, our method improves the near-distribution novelty detection by 6% and passes the state-of-the-art by 1% to 5% across nine novelty detection benchmarks. The code repository is available at <https://github.com/rohban-lab/FITYMI>.

1 Introduction

In novelty detection (ND)¹, the objective is to identify test-time samples that are unlikely to come from the training distribution [1]. Such samples are called anomalous, while the training set is referred to as normal. Recently, PANDA [2] and CSI [3] have considerably pushed state-of-the-art and achieved more than 90% AUROC on the CIFAR-10 dataset [4] in the ND task, where one class is assumed to be normal and the rest are considered anomalous. However, these methods struggle to achieve a similar performance in situations where outliers are semantically close to the normal distribution. That is, they experience a performance drop when faced with such inputs. In this paper, our focus is on the near novelty detection (near-ND), which is a more challenging task and has been explored to a smaller extent. Near novelty detection has found several important practical applications in diverse areas such as medical imaging, and face liveness detection [5].

¹In the literature novelty detection and anomaly detection are used interchangeably. We use the term novelty detection (ND) throughout this paper.

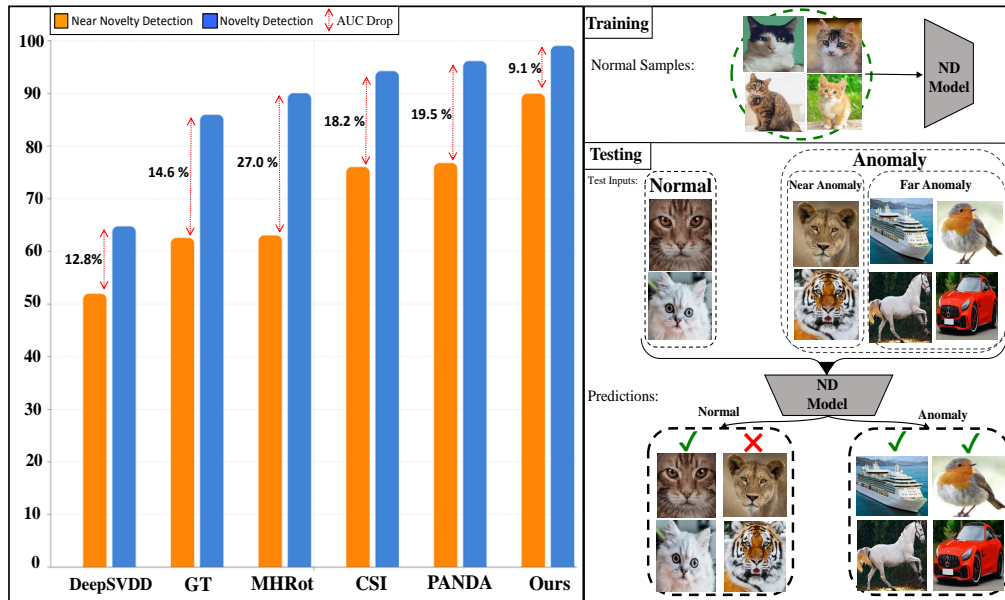


Figure 1: Sensitivity of state-of-the-art anomaly detectors when differences between normal and anomalous samples are subtle. For each model, its performance in detecting far (Blue) and near (Orange) outliers has been reported. Assuming one class of CIFAR-10 is considered normal, the rest of the classes are considered far anomalies, and the semantically nearest class of CIFAR-100 to the normal class is the source of near anomalies (based on the bottom-1 metric, see sec. 2.) A considerable performance drop happens for the most recent methods, which means the learned normal boundaries are not tight enough and need to be adapted. For instance, while some might be able to distinguish a cat image from a car, they are still unable to detect tiger or lion images as anomalies.

Our first contribution is to provide a definition for the near-ND task and benchmark eight recent novelty detection methods in our near-ND setting. Our results reveal a significant performance drop of such approaches for the near-ND setting, despite their excellent results on the standard novelty detection tasks. Fig. 1 compares the performance of PANDA [2] and CSI [3] in the near-ND and ND setups, which shows roughly a 20% AUROC drop. Furthermore, while MHRot [6] performs relatively comparable to PANDA and CSI in ND, it is considerably worse in near-ND, highlighting the need for a near novelty detection benchmark.

A similar problem setup has recently been investigated in the out-of-distribution (OOD) detection domain, which is known as “near out-of-distribution” detection [7]. Out-of-distribution detection and ND are closely related problems with the primary difference being that the normal data constitutes a single class in ND, and multiple classes in out-of-distribution detection. However, out-of-distribution detection models are susceptible to making false detections on anomalous samples that slightly deviate from the normal data. To cope with the challenge in the out-of-distribution detection domain, [7], [6], and [8] employ outlier exposure techniques, i.e., exposing the model to the real outliers, available on the internet, during training. Alternatively, some approaches [9, 10] utilize GANs to generate outliers.

In spite of all these efforts, the issue of nearly anomalous samples has not been studied in the context of ND tasks (i.e., one-class classification). The challenge in the case of ND is that in most cases, the normal data constitutes less conceptual diversity compared with the out-of-distribution detection setup, making the uncertainty estimation challenging, especially for the nearly abnormal inputs. One has to note that some form of uncertainty estimation is required for ND and out-of-distribution detection. This makes near-ND an even more difficult task than near-OOD detection. To deal with this difficulty, we propose to utilize generative models to craft diverse anomalous data. Unfortunately most generative models suffer from (1) instability in the training phase, (2) poor performance on high-resolution images, and (3) low diversity of generated samples [11]. These challenges have prevented their effective use in ND.

To address the mentioned challenges, we propose to use a “non-adversarial” anomaly data generation method. Hence, our second contribution is shedding light on the capabilities of the recently proposed SDE-based generative models [12], in the ND domain. By providing comprehensive experiments and visualizations, we show that a prematurely trained SDE-based model can generate *diverse* and *non-noisy* near-outliers, which considerably beat samples that are generated by GANs or obtained from the available datasets. Interestingly, the methods that employ outlier exposure, such as [6] and [8], show a large performance drop of roughly 15% when faced with our generated anomalous samples. This validates our assertion that the outlier exposure technique is incapable of detecting close outlier samples. Finally, our last contribution is to show that fine-tuning simple baseline ND methods with the generated samples to distinguish them from the normal data leads to a performance boost for both ND and near-ND. The nine benchmark datasets span a wide variety of applications and anomaly granularity. Our method achieves state-of-the-art results in the ND setting, and is especially effective for the defined near-ND setting, where we improve over existing work by a large margin up to 6%.

2 Near Novelty Detection Definition

The problem of *Novelty Detection* for one-class classification is defined using the following setup. Consider \mathcal{X} and \mathcal{Y} be the input and output spaces respectively and let \mathcal{P} be a distribution over $\mathcal{X} \times \mathcal{Y}$. Suppose \mathcal{F} to be a neural network trained on the samples drawn from \mathcal{P} to output a feature representation, which is used to predict the novelty score of an input sample. Let $\mathcal{D}_{\text{Normal}}$ to be the marginal distribution of \mathcal{P} for \mathcal{X} . ND aims to define a decision function \mathcal{G} , demonstrating the following behavior for an arbitrary given test input $x \in \mathcal{X}$:

$$\mathcal{G}(x, \mathcal{F}) = \begin{cases} 0 & \text{if } x \sim \mathcal{D}_{\text{Normal}}, \\ 1 & \text{otherwise.} \end{cases} \quad (1)$$

For ND $|\mathcal{Y}|$ is set to 1, while for out-of-distribution detection and open-set recognition is > 1 .

To provide a standard benchmark for the near-ND task there is a need to define a one-class distribution closeness score. Suppose a K -class training dataset is given from which a normal class C_i is randomly sampled and used to train the model \mathcal{M} . The closest abnormal distribution with respect to the selected normal class for \mathcal{M} can be defined as $C_j \neq C_i$ that minimizes the test time performance when it is considered as the abnormal distribution. We call the performance in the mentioned scenario the bottom-1 score of class C_i with the backbone \mathcal{M} . However, this score depends on the choice of \mathcal{M} , making it specific for every problem setup and method. Therefore, inspired by the CLP criterion introduced in [13] as a measurement of dataset distance, we could use CLP as an alternative closeness score for the novelty detection task.

Given a K -class training dataset, one category is randomly selected as the normal distribution. Then, a supervised classifier \mathcal{P} is trained on the rest $K - 1$ abnormal categories. Assume x to be a training sample of the selected normal class. The closeness score of each abnormal class i with respect to the normal class is obtained as follows:

$$\text{Closeness score}_i = \sum_{x \in \text{Normal Class}} \mathcal{P}(\hat{y} = i|x). \quad (2)$$

The higher the closeness score of an abnormal category, the more similar it is to the normal class. The same situation also holds when abnormal categories are selected from another dataset. Fig. 1 in the Appendix indicates a decent correlation between the bottom-1 score and closeness score, implying that our proposed criterion can be considered as a proxy for the ideal score.

3 Proposed Near-Novelty Detection Method

We introduce a two-step training approach, which even can be employed to boost the performance of most of the existing SOTA models. Following the current trend in the field, we start with a pre-trained feature extractor as [14, 15, 2] have shown their effectiveness. We use a ViT [16] backbone since [7] has demonstrated its superiority on the near out-of-distribution detection. In the first step, a fake dataset is generated by a SDE-based model. We quantitatively and qualitatively show that generated

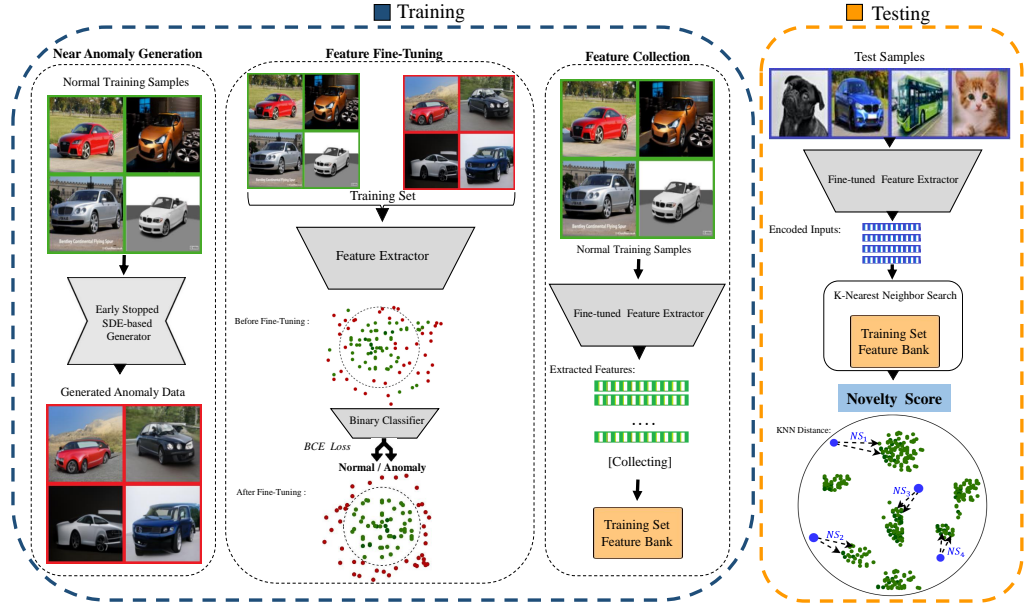


Figure 2: Overview of our framework for near distribution novelty detection. In the first step, the SDE generates semantically close outliers. As it is shown, they have very subtle yet semantic differences with the normal data distribution. After that, using a linear layer, a pre-trained feature extractor is fine-tuned to solve a binary classification between the normal and abnormal inputs. This modifies the normal boundaries toward including more distinctive features. Finally, normal embeddings are stored and used to compute the k -NN distance at the test time.

fake outliers are high-quality, diverse, and yet with semantic differences compared to normal inputs. In the second step, the pre-trained backbone is fine-tuned by the generated dataset and given normal training samples through solving a binary classification loss. Finally, all the normal training samples are passed to the fine-tuned feature extractor, and their embeddings are stored in a memory, which is further used to obtain the k -NN distance of each test input sample.

3.1 Training Phase

Step 1 : Near Anomaly Generation In order to generate near anomalous samples, the SDE-based model proposed in [12] is adapted for the novelty detection task. In the SDE, the gradient of the logarithmic probability density of the data with respect to the input is called the score. A SDE model considers a continuum of distributions that develop over time in accordance with a diffusion process, rather than perturbing the data with a restricted set of noise distributions. The model is trained to learn how to gradually transform the noisy image back to its original form. The procedure that gradually transforms a data point into random noise is controlled by a pre-determined stochastic differential equation that does not contain any trainable parameters. Finally, inverting this process allows us to seamlessly transform random noise into the data that could be used for sample generation as follows:

$$\begin{aligned} x_{n-1} - x_n &= [f(x, t) - g^2(t)\nabla_x \log p_t(x)]dt + g(t)d\hat{w} \\ x_T &\sim N(0, 1), \end{aligned} \quad (3)$$

where f and g are called the drift and diffusion coefficients respectively. For more details see [12]. The main benefit of using a score-based generative model is that in the backward process (Eq. 3), the score function denoises the input gradually that results in a relatively smooth decline in the FID across training epochs. This enables us to stably produce near anomalous samples based on the FID score of the generated outputs, which could be achieved by stopping the training process earlier than the stage where the model achieves its maximum performance. This is empirically assessed in Fig. 3. Note that a totally different training trajectory is obtained in GANs, where the FID oscillates and premature training does not necessarily produce high-quality anomalous samples. That is why methods like OpenGAN rely on a validation outlier dataset to determine where to stop.

Step 2 : Feature Fine-tuning and Collection Having generated a high-quality fake dataset, a lightweight projection head is added to the feature extractor, and the whole network is trained to solve a binary classification task between the given normal and abnormal inputs. This way, normal class boundaries are tightened and adjusted according to the abnormal inputs. After the training, all the normal embeddings are stored in the memory \mathcal{M} that is used at the test time for assigning abnormality score to a given input.

3.2 Testing Phase

At the test time, for each input x , its k nearest neighbours are found in the \mathcal{M} , which are shown by $m_x^1, m_x^2, \dots, m_x^k$. Finally, the novelty score is found as follows:

$$\text{Novelty Score}(x) = \sum_{n=1}^k \|x - m_x^n\|^2 \quad (4)$$

As the equation shows, the more the novelty score the more likely an input to be anomaly. We use $k = 2$ in our experiments.

4 Settings

Training Details. We use a ViT-B_16 as the feature extractor (pretrained on ImageNet 21k), learning rate = 4e-4, weight decay = 5e-5, batch size = 16, optimizer = SGD, a linear head with 2 output neurons. We freeze the first six layers of the network and the rest is fine-tuned till convergence for all the experiments. For the data generation phase, we use the SDE-based model explained in [12] with exactly the same setup. The inputs are resized to 224, and the data generation stops on FID ≈ 40 and FID ≈ 200 for low and high-resolution datasets. All the results in our tables are either reported from the reference papers or run by us using their official repositories.

Datasets. Following previous works, we evaluate the methods on standard datasets CIFAR-10 [4], CIFAR-100 [4] and extend the results on small and fine-grained datasets FGVC-Aircraft [17], Birds [18], Flowers [19], Stanford-Cars [20], MVTEC-AD [21], WBC [22], and Weather [23]. For the full dataset descriptions and details see the Appendix. Following the standard ND protocol, multi-class datasets are converted into an anomaly detection task by setting a class as normal and all other classes as anomalies. This is performed for all classes, in practice turning a single dataset with C classes into C datasets [14, 24, 2]. For the Near-ND setup, each class of CIFAR-10 (C_i^{10}) and its closest class in CIFAR-100 (C_i^{100}) are selected. Then the model is trained on the training samples of (C_i^{10}) and tested against the aggregation of (C_i^{100}) and (C_i^{10}) test sets. Finally, the average AUROC result across the dataset is reported.

5 Ablation Studies

Sensitivity to Backbone Replacements. Table 1 shows our method sensitivity to the backbone replacements. All the backbones are obtained and used as in [7]. The results are provided for both the ND and near-ND evaluation setups. For each backbone, the performance with and without the feature fine-tuning phase is reported, showing a consistent improvement across different architectures. The performance boost is surprisingly large for some backbones such as ResNet-152, ViT-B_16, and R50+ViT-B_16 with roughly 16% , 25%, and 36% boosts in the near-ND setting. Moreover, ViT-B_16 and R50+ViT-B_16 perform roughly 8% and 16% better after the fine-tuning in the ND setup, showing the *generality* of our approach regardless of the setting or backbone. This mainly happens because of the diverse yet semantically close generated outliers that are used to modify the learned normal class boundaries.

SDE vs. GAN. In this experiment, the one-vs-all setting is employed on the WBC dataset. Table 2 shows clear superiority of using a SDE-based model compared to the well-known StyleGAN2-ADA [25] with 4% to 10% better performance based on the chosen normal class. Evidently, employing our fake samples generated by the SDE is almost always beneficial in spite of the ones generated

Table 1: The effectiveness of our approach over different backbones (in AUROC %) in the ND (far) and near-ND (near) settings. The results show consistent improvements regardless of the backbone or setting that is used.

Setting	Dataset	Training	Models				
			ResNet-152	ViT-B_16*	ViT-B_32†	R50+ViT-B_16*	ConvNeXt-B†
ND	CIFAR-10	Before	92.5	91.0	95.3	82.2	97.1
		After	95.3	99.1	98.3	98.8	97.8
near-ND	CIFAR-10vs100	Before	58.5	65.5	66.3	50.0	71.5
		After	74.7	90.0	78.9	85.9	81.1

* Pretrained on ImageNet 21K.

† Pretrained on ImageNet 21K and finetuned on ImageNet 1K.

by StyleGAN2-ADA. Interestingly, StyleGAN samples are harmful to the performance in class 2, significantly reducing the performance by 7%.

Having artifacts, mode-collapse, and undiversified generated samples could be the reasons behind this observation, which are shown in Appendix (Fig. 2). This highlights that not all the generative models are beneficial for the ND and near-ND tasks, and they need to be carefully selected based on the constraints defined in such domains.

Table 2: Comparison of our model performance (in AUROC %) upon using different generative models for each class of the WBC dataset. The performance of the model base backbone is also included to measure the effectiveness of the training process. Score-based data generation considerably passes the GAN-based SOTA in the novelty detection task.

Dataset	Generative Model	Labels				
		1	2	3	4	Mean
WBC	Base Backbone	88.8	96.8	70.2	76.6	83.1
	StyleGAN2-ADA	90.5	89.7	82.4	78.6	85.3
	SDE	94.8	96.5	87.8	88.9	91.2

Sensitivity to k -NN and Stopping Point. Table 3 shows the performance stability with respect to the number of nearest neighbours for both the ND and near-ND setups. Clearly, the method is barely sensitive to this parameter. DN2 [26] has provided extensive experiments on the effectiveness of applying k -NN to the pre-trained features for the AD task, claiming $k = 2$ is the best choice. We also observe that the same trend happens in our experiments. Similarly, the method is robust against

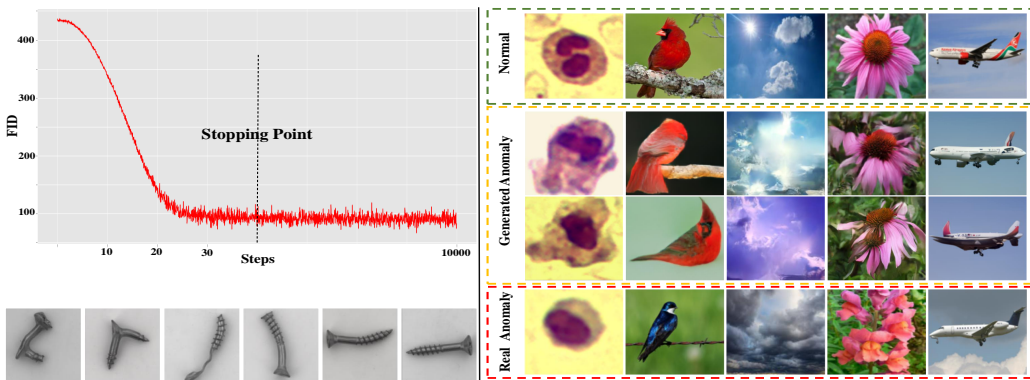


Figure 3: The process of abnormal data generation utilizing the SDE model is shown. On the left, the fake samples evolve during the generation phase. Thus, obtaining high-quality samples is feasible by early stopping. On the right, some generated samples of different datasets as well as their corresponding real anomalies are shown.

the stopping point with at most 2% variation for reasonable FID scores, making it practical for the real-world applications.

Table 3: The sensitivity of the proposed method to the k -NN parameter and stopping point based on the FID score.

Setting	Dataset	KNN					Stopping Point			
		k=1	k=2	k=5	k=10	k=50	300<FID	100<FID<200	30<FID<50	FID<20
ND	CIFAR-10	99.0	99.1	98.9	98.9	98.7	96.8	97.7	99.1	92.6
near-ND	CIFAR-10vs100	89.8	90.0	90.0	90.0	89.7	82.7	87.1	90.0	68.2

CIFAR-10-FSDE Benchmark. To further show the quality of the proposed generated dataset, we evaluated the performance of some of the most outstanding methods when the generated dataset is considered as anomalous at the test time. We call the dataset CIFAR-10-FSDE. For the ND methods such as [2, 8, 3], one class of CIFAR-10 is randomly sampled as normal and the test set is made using the corresponding test samples of the normal class and a random subset of the fake dataset with the same size as anomalies. For the OOD detection methods such as [6] the entire CIFAR-10 is considered normal and a subset of the fake dataset equal to the entire CIFAR-10 test set forms anomalies.

As Table 4 represents, most of the methods significantly fail to detect our fake samples, which is particularly the case for PANDA [2] with 40% performance drop. Surprisingly, OE and DeepSAD with roughly 15% and 30% performance decrease do not work decently despite being exposed to real outliers during the training process. It is worth noticing that CSI [3] shows the least performance drop roughly 7%, revealing that SSL-based methods produce high quality features compared to either pre-trained or semi-supervised approaches in the ND task.

Table 4: The performance of novelty detection methods (AUROC %) on our Cifar-10-FSDE dataset that consists of images generated using the proposed method on the CIFAR-10 dataset. Each model is trained according to its corresponding setting, except its test-time anomalies are replaced by our fake samples.

Dataset	OOD (Multi-Class)		ND (One-Class)					
	OpenGAN [†]	OE [†]	DeepSAD [†]	GT	CSI	PANDA*	MSAD*	Transformaly*
CIFAR-10-FSDE	88.4	78.2	53.4	60.5	87.4	57.7	64.1	75.0

* Pretrained on ImageNet.

[†] Require extra Dataset.

5.1 Comparisons with state-of-the-art

In this section, we compare our method with the most outstanding SOTAs methods in the ND and NND setups. we have used the official implementations and produced the results for all the methods in the near-ND setup. To provide a fair comparison, we compare our method to all the recently proposed methods regardless of being published. For instance, Transformaly and MSAD are not published yet while obtaining the SOTA results. All the experiments are performed 10 times and the average is reported.

Comparison on Standard Datasets. We compare our approach with the top current self-supervised and pre-trained feature adaptation methods in the ND [3, 2, 24, 27, 6]. Results that were reported in the original papers were copied. When the results were not reported in the original papers, we ran the experiments (where possible). Table 5 shows our method surpasses the previous state-of-the-art on the standard benchmark while passing it by roughly 6% in the near-ND setup. Note that except CSI, all the other SOTA approaches employ a pre-trained architecture, particularly Transformaly [27], that utilizes a ViT backbone. However, due to the feature fine-tuning phase of our approach, the borders of the normal samples become well-structured, thus better representing the normal semantic features.

Small and Fine-grained Datasets. To further represent the effectiveness of our approach, it is evaluated on harder tasks such as fine-grained novelty detection and small datasets that do not

Table 5: The performance of novelty detection methods (AUROC %) in the ND setting on various datasets. Our method achieves the SOTA or considerably pass it on almost all the datasets.

(a) ND Setting

Setting	Datasets	Pre-trained				
		From Scratch	PANDA	MSAD	Transfornaly	Ours
		(ResNet-18)	(ResNet-152)	(ResNet-152)	(ViT-B_16)	(ViT-B_16)
ND	Birds	52.4	95.3	96.7	97.8	98.5
	Stanford-Cars	66.5	87.6	89.1	86.7	89.8
	CIFAR-10	94.3	96.2	97.2	98.3	99.1
	CIFAR-100	89.6	94.1	96.4	97.3	98.1
	Flowers	60.8	94.1	96.5	99.9	99.9
	FGVC-Aircraft	64.6	77.7	79.8	84.0	88.7
	MvTecAD	63.6	86.5	87.2	87.9	86.4
	WBC	50.4	87.4	87.0	85.1	91.2
	Weather	91.5	81.5	92.4	94.3	97.0

(b) The performance of the SOTA novelty detection methods compared to ours in AUROC % in the near-ND and ND settings. In the near-ND setup, the normal class is considered a class of CIFAR-10, and the closest abnormal distribution in CIFAR-100 forms the abnormal distribution. OpenGan is adapted for the one-class setting. While Transfornaly, PANDA, and CSI achieve very close results in the ND setup, they work significantly differently in the near-ND setting, highlighting the importance of having an near-ND benchmark.

Setting	Dataset	From Scratch				Pre-trained				
		GT	MHRot	CSI	one-class OpenGan	DN2	PANDA	MSAD	Transfornaly	Ours
ND	CIFAR-10	86.0	90.1	94.3	83.6	92.5	96.2	97.2	98.3	99.1
near-ND	CIFAR-10vs100	62.6	63.1	76.1	50.0	58.5	76.8	79.5	84.1	90.0

contain enough normal diversity. As Table 5 shows, we achieve SOTA results on Birds, Flowers, Stanford-Cars, and MVTEC-AD while passing it by a large margin of 4.7% compared to Transfornaly and 10% compared to PANDA on Airplane. We also considerably pass the SOTA by roughly 4% on both WBC and Weather datasets.

As Table 5 shows, our proposed method is effective for this setup and improves the SOTA by roughly 6% compared to Transfornaly and 14% compared to PANDA. To further validate our method, we adapt OpenGAN to novelty detection and report its near novelty detection results. Surprisingly, even by employing fake abnormal samples generated by a GAN and being exposed to real outliers, it is not able to achieve a decent performance, which again supports the benefits of our proposed approach for generating near distribution abnormal samples.

Synthetic Novelty Detection. While the anomalous data generated by StyleGAN does not fit the fine-tuning phase due to the mentioned problems, they contain lots of artifact-full and distorted samples that a practical novelty detector is expected to detect. Table 6 compares our method with other SOTA methods. Due to learning more distinguishing features, we pass the SOTA by 12%, showing the applicability of our approach in detecting a wide range of anomalies.

Table 6: The performance of SOTA methods on the samples generated by StyleGAN2. The results reveal that regardless of employing an SSL loss with heavy augmentations or pre-trained features, fine-tuning the model with near outliers better forms the normal boundaries.

Dataset	Methods				
	CSI	PANDA	MSAD	Transfornaly	Ours
Cifar-10-FSGAN	83.1	66.1	69.4	82.2	95.1

6 Related Work

Outlier Exposure Based Approaches Utilizing the fake data for the novelty detection task has previously been considered. The general idea is to employ synthetic images, which may be generated by GANs, to augment the training set [28–32]. In the case of open-set recognition, [9] proposed OpenGAN, which adverserially generates fake open-set images. The discriminator is then utilized at the test time for the novelty detection. The key point in OpenGAN is that a tiny additional dataset, containing both in- and outliers, is used as a validation set for the model selection. This, also known as outlier exposure, is necessary due to the GAN unstable training. Along the same line of work, [10] considered generation of fake data in the one-class setting. Specifically, the fake anomalous data is generated through early stopping of a GAN that is trained on the normal samples. They subsequently train a binary classifier on the augmented dataset, to discriminate the normal and generated fake samples. This classifier is later utilized for anomaly detection at the inference time. Even though these models can work well on simple datasets, they cannot handle more complex datasets and cannot detect hard near-distribution anomalies.

It is shown in [7] that by exploiting the pre-trained vision transformers that are fine-tuned on the in-distribution dataset, one can boost near out-of-distribution detection results. They also demonstrated that additional outlier samples improve results even further. Finally, it has to be noted that similar relevant concepts to the near out-of-distribution detection has been explored in other fields e.g. adversarial robust training [33–35].

Self-supervised learning Many studies have shown that Self-supervised methods can extract meaningful features that could be exploited in the anomaly detection tasks such as MHRot [6]. GT [36] uses geometric transformations including flip, translation, and rotation to learn normal features for anomaly detection. Alternatively, puzzle solving [37], and Cut-Paste [38] are proposed in the context of anomaly detection. It has recently been shown that contrastive learning can also improve anomaly detection [3], which encourages the model to learn normal features by contrasting positive, and certain negative samples. The authors claim that negative samples should be made by applying certain transformations that tend to drastically change the data distribution (e.g. rotation).

Pre-trained Methods Several works used pre-trained networks as anomaly detectors. Intuitively, abnormal and normal data do not overlap in the feature space because many features model high-level and semantic image properties. So, in the pre-trained feature space, one may classify normal vs. anomaly. [26] used the k -nearest neighbors distance between the test input and training set features as an anomaly score. [39] trained a GMM on the normal sample features, which could then identify anomalous samples as low probability areas. PANDA [2] attempts to project the pre-trained features of the normal distribution to another compact feature space employing the DSVDD [40] objective function. In [27, 15, 14], the pre-trained model is a teacher and the student is trained to mimic the teacher’s behavior solely on the normal samples. Then, the discrepancy between the teacher and student networks reveal anomalies.

7 Social Impacts

The goal of this study is to increase the safety of modern machine learning models. This will benefit a wide range of fields and activities in society. We believe that novelty detection is used in a variety of areas, including financial services (for example, fraud detection), manufacturing (for example, failure detection), and health care (e.g., unseen disease identification). We intend to offer machine learning researchers an easy-to-use tool that provides safety against a wide range of anomalous data in the real world applications through our study and the release of our code. While we do not expect our effort to have any negative implications, we hope to continue to build on our method in future work.

8 Conclusion

In this paper, we revealed a key weakness of existing SOTA novelty detection methods, where they fail to identify anomalies that are slightly different from the normal data. We proposed to take a non-adaptive generative modeling that allows controllable generation of anomalous data. It turns out that SDEs fit this specification much better compared to other SOTA generative models such as GANs.

The generated data levels up pre-trained distance-based novelty detection methods not only based on their AUROCs in the standard ND setting but also in the near-ND setting. The improvements that are made by our method are consistent across wide variety of datasets, and choices of the backbone model.

References

- [1] Mohammadreza Salehi, Hossein Mirzaei, Dan Hendrycks, Yixuan Li, Mohammad Hossein Rohban, and Mohammad Sabokrou. A unified survey on anomaly, novelty, open-set, and out-of-distribution detection: Solutions and future challenges. *arXiv preprint arXiv:2110.14051*, 2021.
- [2] Tal Reiss, Niv Cohen, Liron Bergman, and Yedid Hoshen. Panda: Adapting pretrained features for anomaly detection and segmentation. In *Proceedings of the IEEE/CVF Conference on Computer Vision and Pattern Recognition*, pages 2806–2814, 2021.
- [3] Jihoon Tack, Sangwoo Mo, Jongheon Jeong, and Jinwoo Shin. Csi: Novelty detection via contrastive learning on distributionally shifted instances. *Advances in neural information processing systems*, 33:11839–11852, 2020.
- [4] Alex Krizhevsky, Geoffrey Hinton, et al. Learning multiple layers of features from tiny images. -, 2009.
- [5] Daniel Pérez-Cabo, David Jiménez-Cabello, Artur Costa-Pazo, and Roberto J López-Sastre. Deep anomaly detection for generalized face anti-spoofing. In *Proceedings of the IEEE/CVF Conference on Computer Vision and Pattern Recognition Workshops*, pages 0–0, 2019.
- [6] Dan Hendrycks, Mantas Mazeika, Saurav Kadavath, and Dawn Song. Using self-supervised learning can improve model robustness and uncertainty. *Advances in Neural Information Processing Systems*, 32, 2019.
- [7] Stanislav Fort, Jie Ren, and Balaji Lakshminarayanan. Exploring the limits of out-of-distribution detection. *Advances in Neural Information Processing Systems*, 34, 2021.
- [8] Lukas Ruff, Robert A Vandermeulen, Nico Görnitz, Alexander Binder, Emmanuel Müller, Klaus-Robert Müller, and Marius Kloft. Deep semi-supervised anomaly detection. *arXiv preprint arXiv:1906.02694*, 2019.
- [9] Shu Kong and Deva Ramanan. Opegan: Open-set recognition via open data generation. In *Proceedings of the IEEE/CVF International Conference on Computer Vision*, pages 813–822, 2021.
- [10] Masoud Pourreza, Bahram Mohammadi, Mostafa Khaki, Samir Bouindour, Hichem Snoussi, and Mohammad Sabokrou. G2d: generate to detect anomaly. In *Proceedings of the IEEE/CVF Winter Conference on Applications of Computer Vision*, pages 2003–2012, 2021.
- [11] Mohammadreza Salehi, Atrin Arya, Barbod Pajoum, Mohammad Otoofi, Amirreza Shaeiri, Mohammad Hossein Rohban, and Hamid R Rabiee. Arae: Adversarially robust training of autoencoders improves novelty detection. *Neural Networks*, 144:726–736, 2021.
- [12] Yang Song, Jascha Sohl-Dickstein, Diederik P Kingma, Abhishek Kumar, Stefano Ermon, and Ben Poole. Score-based generative modeling through stochastic differential equations. *arXiv preprint arXiv:2011.13456*, 2020.
- [13] Jim Winkens, Rudy Bunel, Abhijit Guha Roy, Robert Stanforth, Vivek Natarajan, Joseph R Ledsam, Patricia MacWilliams, Pushmeet Kohli, Alan Karthikesalingam, Simon Kohl, et al. Contrastive training for improved out-of-distribution detection. *arXiv preprint arXiv:2007.05566*, 2020.
- [14] Mohammadreza Salehi, Niousha Sadjadi, Soroosh Baselizadeh, Mohammad H. Rohban, and Hamid R. Rabiee. Multiresolution knowledge distillation for anomaly detection. In *Proceedings of the IEEE/CVF Conference on Computer Vision and Pattern Recognition (CVPR)*, pages 14902–14912, June 2021.
- [15] Paul Bergmann, Michael Fauser, David Sattlegger, and Carsten Steger. Uninformed students: Student-teacher anomaly detection with discriminative latent embeddings. In *Proceedings of the IEEE/CVF Conference on Computer Vision and Pattern Recognition*, pages 4183–4192, 2020.
- [16] Alexey Dosovitskiy, Lucas Beyer, Alexander Kolesnikov, Dirk Weissenborn, Xiaohua Zhai, Thomas Unterthiner, Mostafa Dehghani, Matthias Minderer, Georg Heigold, Sylvain Gelly, et al. An image is worth 16x16 words: Transformers for image recognition at scale. *arXiv preprint arXiv:2010.11929*, 2020.
- [17] S. Maji, J. Kannala, E. Rahtu, M. Blaschko, and A. Vedaldi. Fine-grained visual classification of aircraft. Technical report, -, 2013.
- [18] Catherine Wah, Steve Branson, Peter Welinder, Pietro Perona, and Serge Belongie. The caltech-ucsd birds-200-2011 dataset. -, 2011.
- [19] Maria-Elena Nilsback and Andrew Zisserman. Automated flower classification over a large number of classes. In *2008 Sixth Indian Conference on Computer Vision, Graphics & Image Processing*, pages 722–729. IEEE, 2008.
- [20] Jonathan Krause, Michael Stark, Jia Deng, and Li Fei-Fei. 3d object representations for fine-grained categorization. In *Proceedings of the IEEE international conference on computer vision workshops*, pages 554–561, 2013.

- [21] Paul Bergmann, Michael Fauser, David Sattlegger, and Carsten Steger. Mvtec ad—a comprehensive real-world dataset for unsupervised anomaly detection. In *Proceedings of the IEEE/CVF conference on computer vision and pattern recognition*, pages 9592–9600, 2019.
- [22] Xin Zheng, Yong Wang, Guoyou Wang, and Jianguo Liu. Fast and robust segmentation of white blood cell images by self-supervised learning. *Micron*, 107:55–71, 2018.
- [23] A Gbeminiyi. Multi-class weather dataset for image classification. *Mendeley Data*, 2018.
- [24] Tal Reiss and Yedid Hoshen. Mean-shifted contrastive loss for anomaly detection. *arXiv preprint arXiv:2106.03844*, 2021.
- [25] Tero Karras, Miika Aittala, Janne Hellsten, Samuli Laine, Jaakko Lehtinen, and Timo Aila. Training generative adversarial networks with limited data. *Advances in Neural Information Processing Systems*, 33:12104–12114, 2020.
- [26] Liron Bergman, Niv Cohen, and Yedid Hoshen. Deep nearest neighbor anomaly detection. *arXiv preprint arXiv:2002.10445*, 2020.
- [27] Matan Jacob Cohen and Shai Avidan. Transformally—two (feature spaces) are better than one. *arXiv preprint arXiv:2112.04185*, 2021.
- [28] Pierrick Chatillon and Coloma Ballester. History-based anomaly detector: An adversarial approach to anomaly detection. In *Proceedings of SAI Intelligent Systems Conference*, pages 761–776. Springer, 2020.
- [29] Hironori Murase and Kenji Fukumizu. Algan: Anomaly detection by generating pseudo anomalous data via latent variables. *arXiv preprint arXiv:2202.10281*, 2022.
- [30] Da-Wei Zhou, Han-Jia Ye, and De-Chuan Zhan. Learning placeholders for open-set recognition. In *Proceedings of the IEEE/CVF Conference on Computer Vision and Pattern Recognition*, pages 4401–4410, 2021.
- [31] Lawrence Neal, Matthew Olson, Xiaoli Fern, Weng-Keen Wong, and Fuxin Li. Open set learning with counterfactual images. In *Proceedings of the European Conference on Computer Vision (ECCV)*, pages 613–628, 2018.
- [32] ZongYuan Ge, Sergey Demyanov, Zetao Chen, and Rahil Garnavi. Generative openmax for multi-class open set classification. *arXiv preprint arXiv:1707.07418*, 2017.
- [33] Stanislav Fort. Adversarial vulnerability of powerful near out-of-distribution detection. *arXiv preprint arXiv:2201.07012*, 2022.
- [34] Jie Ren, Stanislav Fort, Jeremiah Liu, Abhijit Guha Roy, Shreyas Padhy, and Balaji Lakshminarayanan. A simple fix to mahalanobis distance for improving near-ood detection. *arXiv preprint arXiv:2106.09022*, 2021.
- [35] Yao-Yuan Yang, Cyrus Rashtchian, Ruslan Salakhutdinov, and Kamalika Chaudhuri. Close category generalization. *CoRR*, abs/2011.08485, 2020.
- [36] Izhak Golan and Ran El-Yaniv. Deep anomaly detection using geometric transformations. *Advances in neural information processing systems*, 31, 2018.
- [37] Mohammadreza Salehi, Ainaz Eftekhari, Niousha Sadjadi, Mohammad Hossein Rohban, and Hamid R Rabiee. Puzzle-ae: Novelty detection in images through solving puzzles. *arXiv preprint arXiv:2008.12959*, 2020.
- [38] Chun-Liang Li, Kihyuk Sohn, Jinsung Yoon, and Tomas Pfister. Cutpaste: Self-supervised learning for anomaly detection and localization. In *Proceedings of the IEEE/CVF Conference on Computer Vision and Pattern Recognition*, pages 9664–9674, 2021.
- [39] Zhisheng Xiao, Qing Yan, and Yali Amit. Do we really need to learn representations from in-domain data for outlier detection? *arXiv preprint arXiv:2105.09270*, 2021.
- [40] Lukas Ruff, Robert Vandermeulen, Nico Goernitz, Lucas Deecke, Shoaib Ahmed Siddiqui, Alexander Binder, Emmanuel Müller, and Marius Kloft. Deep one-class classification. In *International conference on machine learning*, pages 4393–4402. PMLR, 2018.

Appendix

A Near-ND

A.1 Comparison between bottom-1 and CLP

In section 2, we proposed the closeness score (CLP) to find the closest abnormal class for each class of the normal dataset. In our experiments, we used the ViT-B_16 (pretrained on ImageNet-21K) as the backbone used for extracting the closest abnormal classes based on this criterion. The bottom-1 abnormal class is the class that has the lowest novelty detection performance during the testing phase. Note that the abnormal classes chosen based on the CLP criterion do not necessarily have the worst novelty detection performance; therefore, it is expected for the novelty detection methods to perform better on the CLP criterion. This section aims to investigate how well these two criteria match each other. In the Table 7, for each novelty detection model and every class of the CIFAR-10 dataset, the bottom-1 class is shown. Furthermore, the last row indicates the closest abnormal class selected based on the CLP criterion. As shown in the Table 7, the extracted classes based on the CLP criterion are the same or conceptually similar to the respected bottom-1 classes. Figure Figure 1 also shows a decent correlation between the bottom-1 score and the CLP score, which means both these criteria could be used to extract near-distribution abnormal classes, and that the CLP could be used as a proxy to the bottom-1 criterion.

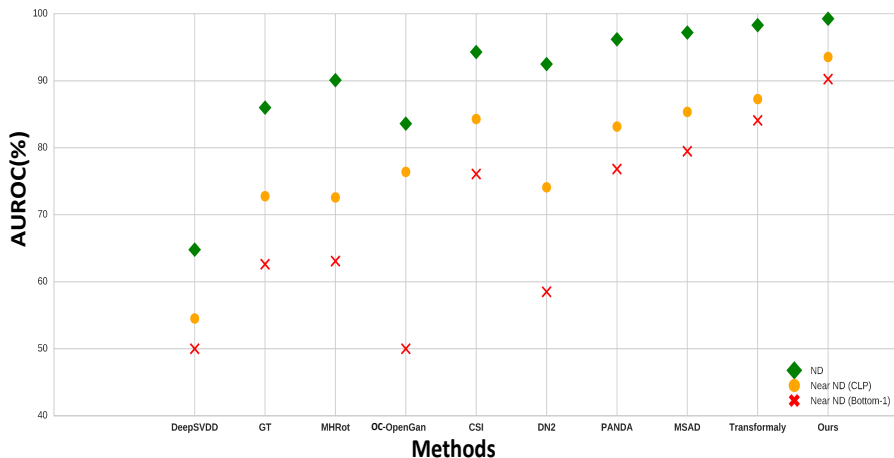


Figure 1: The performance of novelty detection methods (AUROC %) in the near-ND and ND settings. In the near-ND setting, results are reported according to both criteria, i.e. CLP and bottom-1.

Table 7: For each model and every class of the CIFAR-10, the anomalous class that minimizes the anomaly detection performance among 100 classes of the CIFAR-100 dataset is reported. The last row is the CIFAR-100 class that achieves the highest CLP score. Note that the latter does not depend on the anomaly detection method.

Method	Airplane	Automobile	Bird	Cat	Deer	Dog	Frog	Horse	Ship	Truck
DeepSVDD	Plain	Plain	Plain	Cloud	Plain	Mountain	Plain	Plain	Plain	Plain
GT	Mountain	Pickup_Truck	Camel	Fox	Elephant	Bear	Crocodile	Elephant	Train	Bus
MHRot	Plain	Pickup_Truck	Camel	Fox	Cattle	Fox	Crocodile	Elephant	Sea	Pickup_Truck
one_class OpenGan	Plain	Plain	Plain	Wardrobe	Forest	Telephone	Aquarium_Fish	Oak_Tree	Whale	Plain
CSI	Pickup_Truck	Pickup_Truck	Camel	Fox	Cattle	Cattle	Dinosaur	Cattle	Pickup_Truck	Pickup_Truck
DN2	Plain	Pickup_Truck	Willow_Tree	Fox	Forest	Fox	Forest	Cattle	Sea	Pickup_Truck
PANDA	Dolphin	Pickup_Truck	Kangaroo	Fox	Kangaroo	Raccoon	Crocodile	Cattle	Bridge	Pickup_Truck
MSAD	Cloud	Pickup_Truck	Kangaroo	Fox	Kangaroo	Fox	Beaver	Cattle	Sea	Pickup_Truck
Transformatly	Cloud	Pickup_Truck	Kangaroo	Rabbit	Kangaroo	Wolf	Lizard	Cattle	Sea	Pickup_Truck
Ours	Tank	Pickup_Truck	Camel	Wolf	Kangaroo	Wolf	Lizard	Camel	Streetcar	Pickup_Truck
CLP	Rocket	Pickup_Truck	Shrew	Leopard	Cattle	Rabbit	Lizard	Cattle	Bridge	Bus

Table 8: The performance of novelty detection methods (AUROC %) in the near-ND setting. For each method and every normal class, both results have been reported according to the CLP and bottom-1 metrics.

Method	Metric	Airplane	Automobile	Bird	Cat	Deer	Dog	Frog	Horse	Ship	Truck	Mean
DeepSVDD	bottom-1	17.2	24.0	22.1	34.0	21.5	25.1	25.8	27.1	32.7	20.4	50.0
	CLP	52.1	52.3	53.9	64.7	53.0	39.9	57.5	55.6	61.7	54.5	54.5
GT	bottom-1	39.2	61.8	61.0	54.2	60.1	65.1	71.0	70.4	80.5	62.9	62.6
	CLP	85.6	61.8	81.4	58.7	61.6	80.2	78.8	76.1	80.6	62.9	72.8
MHRot	bottom-1	34.1	62.4	65.2	57.6	61.9	69.3	77.8	73.1	75.0	54.3	63.1
	CLP	77.4	62.4	81.5	60.4	61.9	82.1	82.3	73.3	79.9	64.7	72.6
one_class OpenGan	bottom-1	11.4	18.1	10.0	15.3	19.2	29.8	16.9	20.9	40.4	6.2	50.0
	CLP	66.3	92.2	94.9	64.7	51.7	63.7	93.3	66.5	85.7	85.0	76.4
CSI	bottom-1	73.4	68.4	81.3	65.0	71.8	78.1	88.3	85.9	91.1	57.5	76.1
	CLP	94.2	68.4	93.7	79.9	71.9	90.6	91.5	87.1	91.0	74.6	84.3
DN2	bottom-1	57.5	61.8	43.8	54.0	51.5	66.2	59.4	74.6	54.9	61.0	58.5
	CLP	87.5	61.8	61.7	66.5	84.4	83.5	74.3	74.6	77.0	69.8	74.1
PANDA	bottom-1	89.8	70.0	81.7	50.0	77.0	74.8	83.8	80.3	88.7	72.1	76.8
	CLP	94.5	70.0	89.1	66.7	91.7	88.8	86.5	80.3	88.7	75.3	83.2
MSAD	bottom-1	90.4	72.0	87.5	52.9	81.1	80.5	85.3	83.0	83.8	78.3	79.5
	CLP	94.0	72.0	89.8	75.3	87.3	94.5	90.2	83.0	88.6	79.0	85.4
Transformaly	bottom-1	84.1	69.5	90.3	78.4	82.9	91.8	87.3	95.1	86.0	75.5	84.1
	CLP	92.1	69.5	91.0	81.1	92.1	95.6	87.3	95.1	92.2	76.7	87.3
Ours	bottom-1	95.6	83.5	93.4	86.9	92.3	84.5	94.8	97.8	93.7	77.0	90.0
	CLP	96.3	83.5	99.2	89.4	97.0	95.8	94.8	98.0	93.8	79.9	92.8

A.2 Bottom- i Classes as the Abnormal Distribution

The Bottom- i means averaging the AUROCs for the i abnormal classes that have the lowest AUROCs, e.g. bottom-100 in the case of CIFAR-100 denotes averaging the AUROC results for all 100 classes.

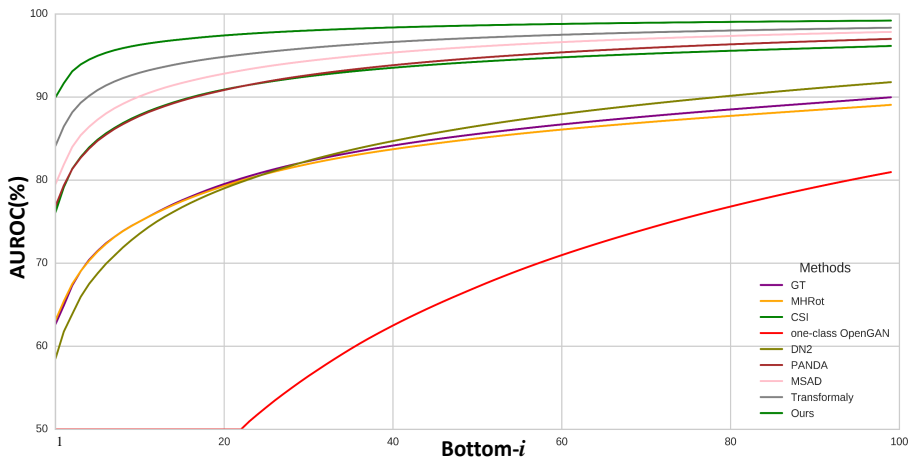


Figure 2: By increasing i , the AUROCs of the models improve due to the presence of more anomalies that are further from the boundary. As expected, in most cases, the gap between the performance of models has become smaller. Furthermore, in the case of $i = 1$, in which anomalies constitute the near distribution ones, the models' performances vary greatly. In this case, our proposed method achieves SOTA results by a large margin.

A.3 Per-Class Results

In this section, we provide our model’s performance for every class of the CIFAR-10 and CIFAR-100 datasets.

Table 9: Performance of our method in AUROC (%) for each class of the CIFAR-10 dataset in the one-vs-all setting.

Method	0	1	2	3	4	5	6	7	8	9	Mean
Ours	99.2	99.4	99.2	98.1	99.5	98.1	99.8	99.5	99.2	98.8	99.1

Table 10: Performance of our method in AUROC (%) for each class of the coarse-grained CIFAR-100 dataset in the one-vs-all setting.

Method	0	1	2	3	4	5	6	7	8	9	10	11	12	13	14	15	16	17	18	19	Mean
Ours	98.0	99.0	99.1	98.2	98.2	97.7	98.8	98.7	99.0	96.6	96.5	98.1	98.4	96.3	98.1	97.1	98.5	98.8	98.8	97.9	98.1

A.4 CIFAR-10 vs. CIFAR-100

In this section, we compare images of the CIFAR-10 dataset, images of respective classes selected from the CIFAR-100 dataset based on the CLP criterion, and the corresponding anomalies generated by our SDE model.



Figure 3: For each class of CIFAR-10, nearest class from CIFAR-100 has been provided, according to the closeness score. In each 3-row panel, the first row is assumed as normal, the second one is assumed the nearest abnormal class, and the third row indicates the corresponding generated fake images using the SDE model.



Figure 4: For each class of CIFAR-10, nearest class from CIFAR-100 has been provided, according to the closeness score. In each 3-row panel, the first row is assumed as normal, the second one is assumed the nearest abnormal class, and the third row indicates the corresponding generated fake images using the SDE model.

B The SDE-based Generative Model

B.1 SDE vs. Other Generative Models

In this section, according to our main setting, we have replaced the SDE with other generative models, and sampled the images generated by these models before convergence. Because in our setup, only one class (the normal class) is available for the training of the generative model. As the sample size becomes limited in such a setting, model convergence and generation of high quality real samples become a challenge. Even under such circumstances, the SDE-based models converge. Furthermore, such models can eventually generate high quality real images. However, other generative models do not converge properly, and the images that are sampled using the early stopped model are often noisy and contain artifacts. As opposed to other generative methods, the proposed premature training of the SDE yields authentic, near-distribution, diverse, and artifact-free images. This makes it a better choice for the near-ND setup.



Figure 5: Generated anomalous samples by different generative models on the FGVC-Aircraft dataset.

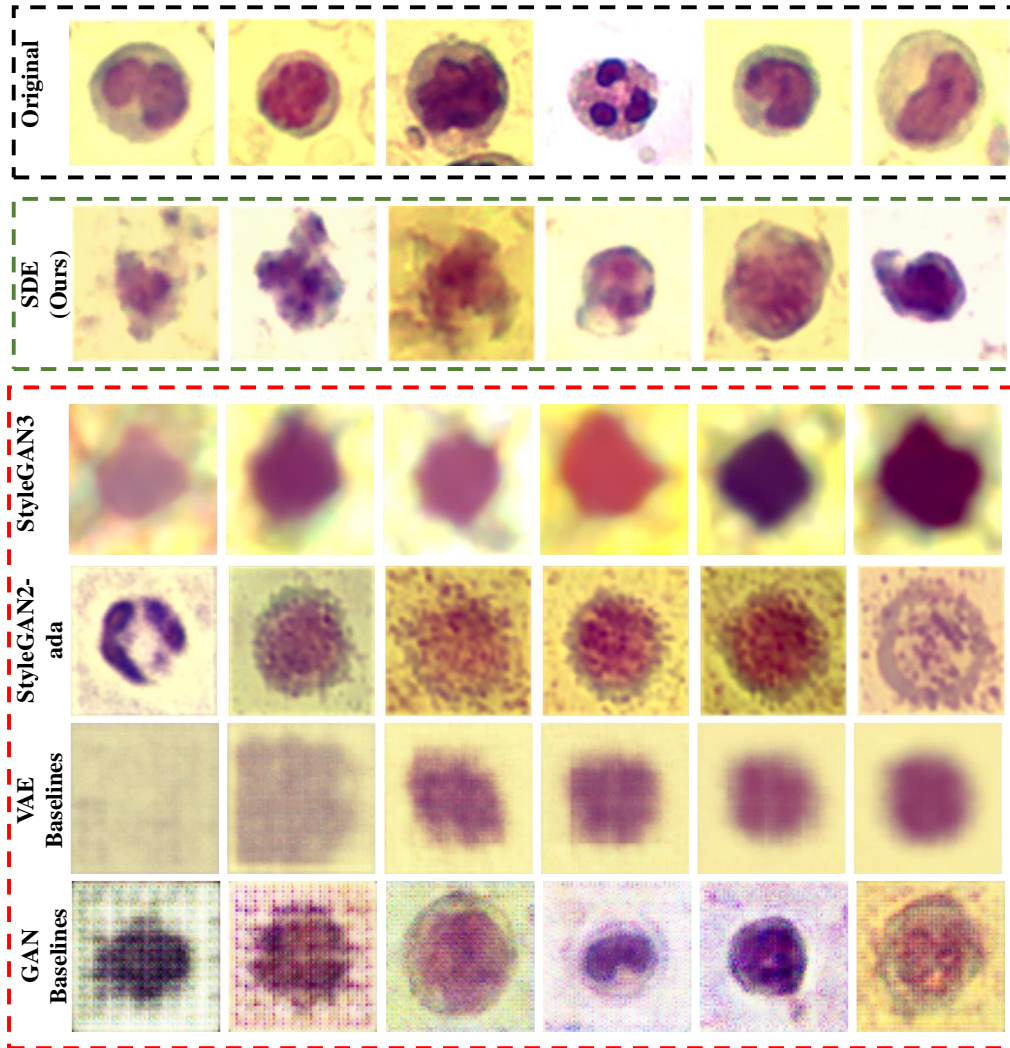


Figure 6: Generated anomalous samples by different generative models on the WBC dataset.

B.2 CIFAR-10-FSDE

These images are randomly plotted for each of the classes in the proposed dataset, CIFAR-10-FSDE, generated through an early stopped SDE. As can be seen, the images are clearly different semantically from the normal class. Despite this semantic difference, most novelty detection models have a poor performance in the detection of these images as anomalous.

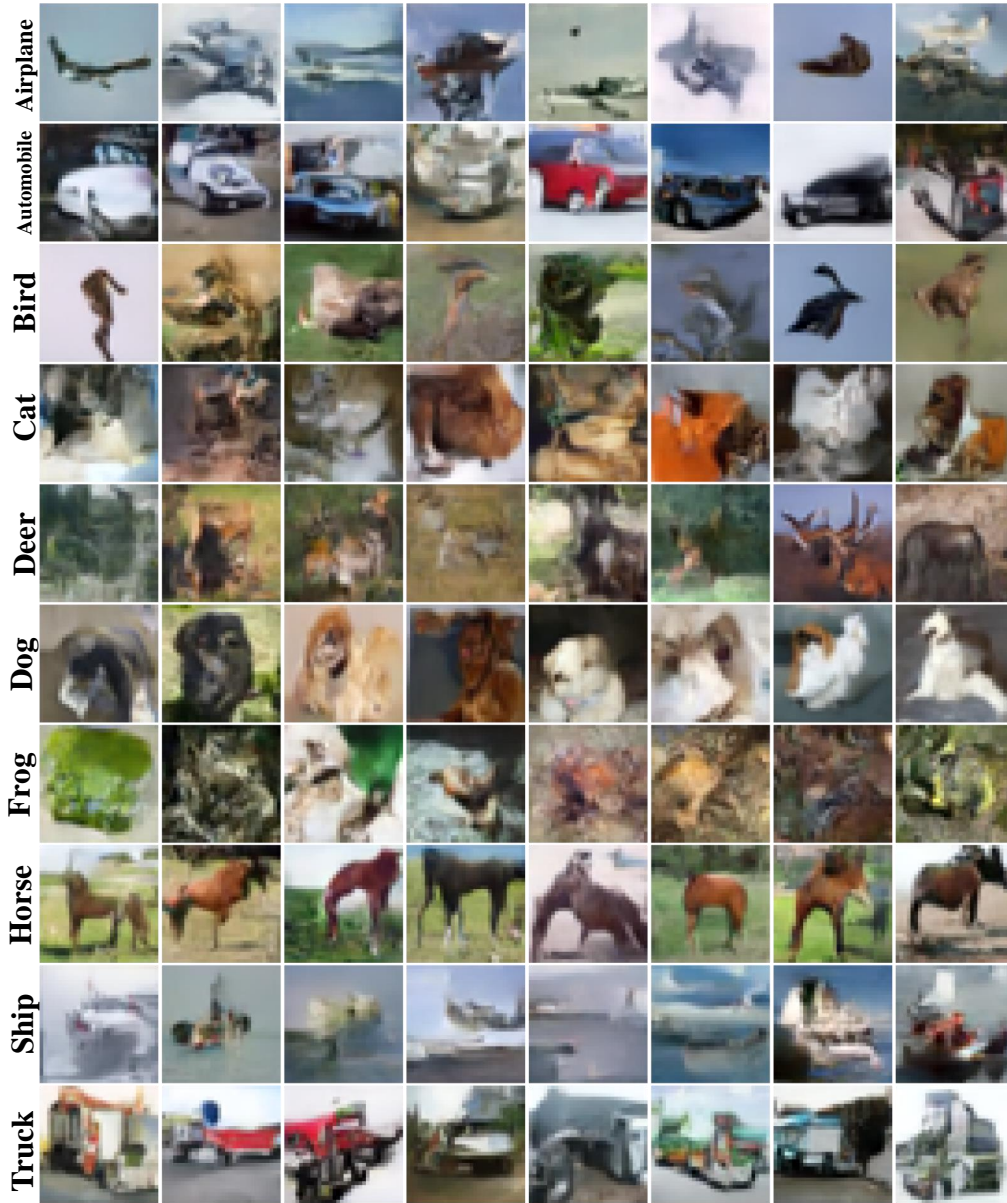


Figure 7: An overview of images in the synthetic CIFAR10-FSDE dataset.

B.3 Overview of Generated Anomaly Images on Various Datasets

Each row is a class on which the SDE model is trained. The SDE model is trained on higher number of iterations in moving from the left to the right columns. The rightmost column contains a real images.

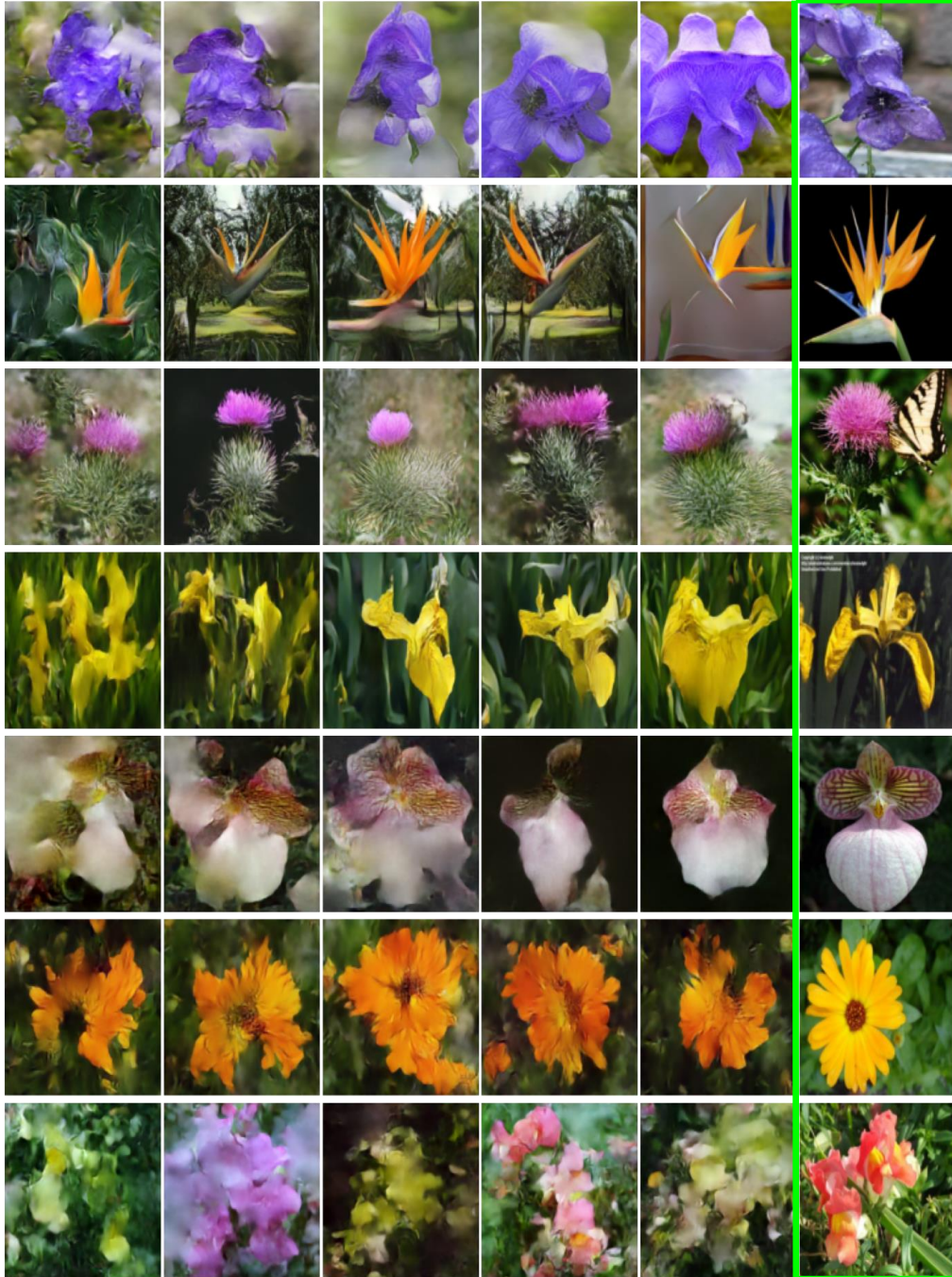


Figure 8: Generated anomaly images on 102 category of the Flowers dataset. The images highlighted in green are normal samples.

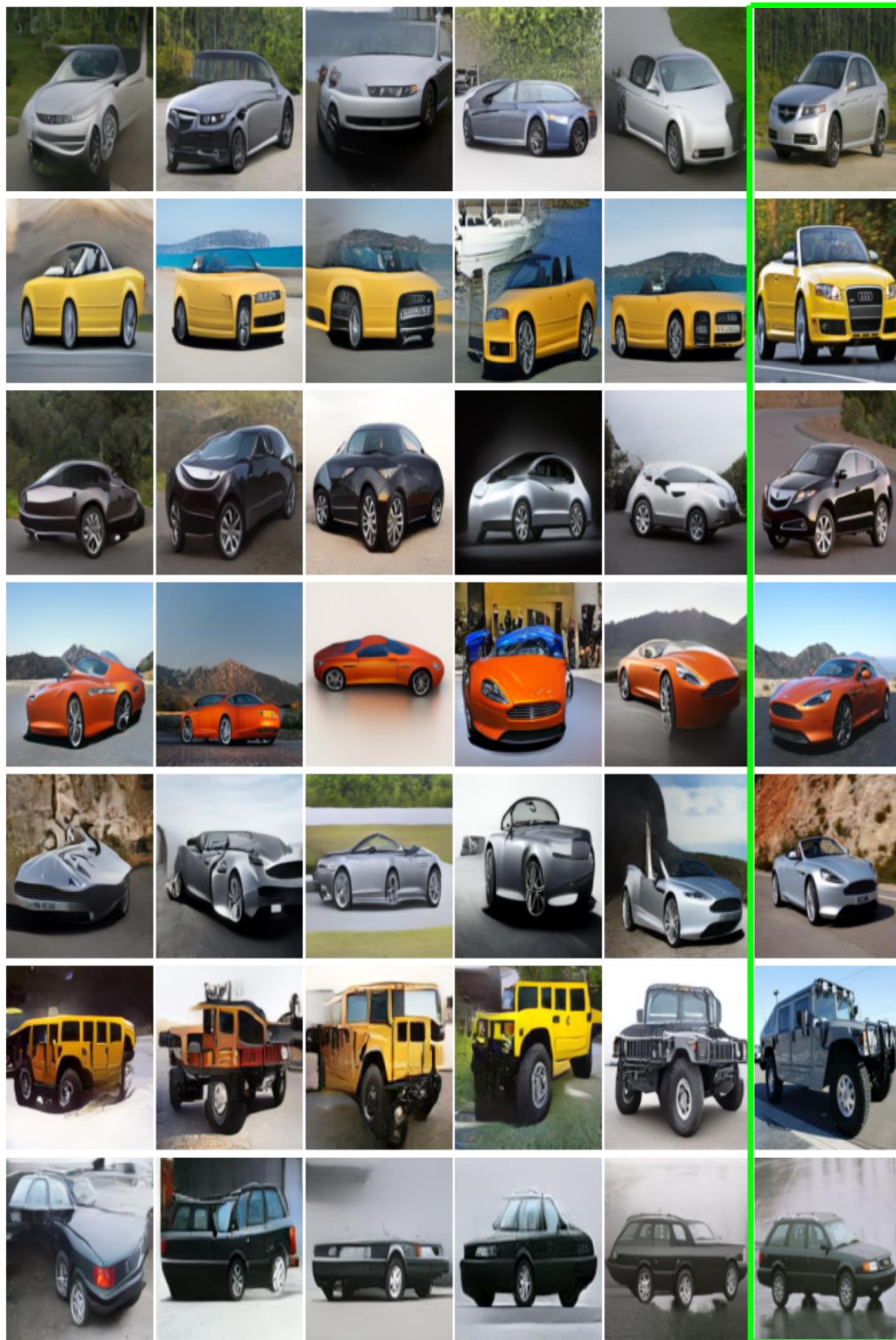


Figure 9: Generated anomaly images on the StanfordCars dataset. The images highlighted in green are normal samples.



Figure 10: Generated anomaly images on the Caltech-UCSD Birds 200 dataset. The images highlighted in green are normal samples.

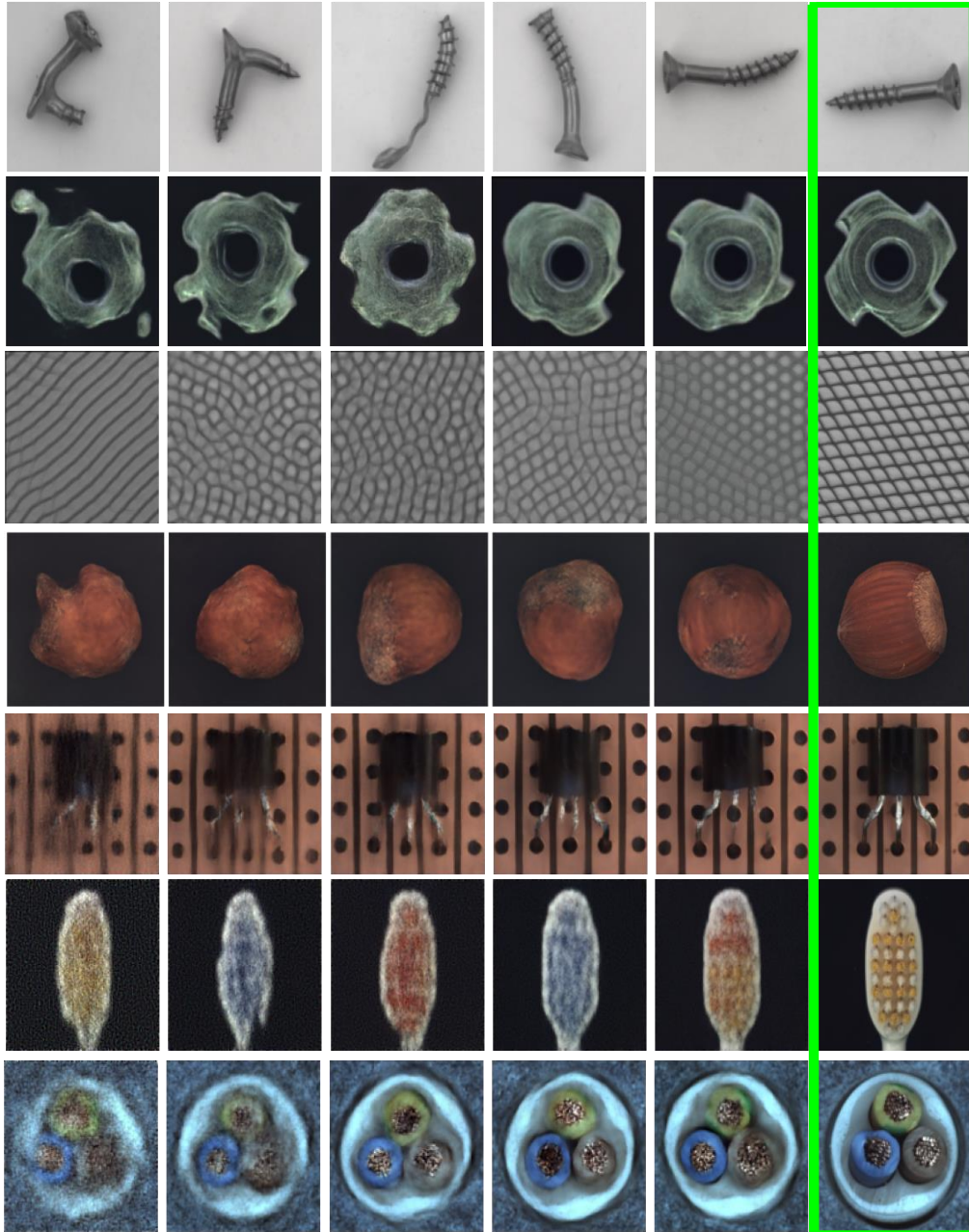


Figure 11: Generated anomaly images on the MVTecAD dataset. The images highlighted in green are normal samples.

C Dataset Descriptions

The setting is reported from [24].

Standard Datasets We evaluate our method on a set of commonly used datasets: CIFAR-10 consists of RGB images of 10 object classes. CIFAR-100: we use the coarse-grained version that consists of 20 classes.

Small datasets To further extend our results, we compared the methods on a number of small datasets from different domains: 102 Category Flowers and Caltech-UCSD Birds 200. For each of these datasets, we evaluated the methods using only each of the first 20 classes as normal, and using the entire test set for the evaluation. For FGVC-Aircraft, due to the extreme similarity of the classes to each other, we randomly selected a subset of ten classes from the entire dataset, such that no two classes have the same `Manufacturer`. Following are the selected classes: [91, 96, 59, 19, 37, 45, 90, 68, 74, 89].

MvTecAD: This dataset contains 15 different industrial products, with normal images of the proper products for training and 1 to 9 types of manufacturing errors as anomalies. The anomalies in MvTecAD are in-class, i.e. the anomalous images come from the same class of the normal images with subtle variations.

Symmetric datasets We evaluated our method on datasets that contain symmetries, such as images that have no preferred angle (microscopy, aerial images): WBC : we used the 4 big classes in “Dataset 1” of the microscopy images of white blood cells, with a 80%/20% train-test split.